Journal of
Marine Science and Engineering

MDPI

Article

Bio-Inspired Cooperative Control Scheme of Obstacle Avoidance for UUV Swarm

Zhao Wang, Hongjian Wang *, Jianya Yuan, Dan Yu, Kai Zhang and Jingfei Ren

College of Intelligent System Science and Engineering, Harbin Engineering University, Harbin 150001, China; 814551366@hrbeu.edu.cn (Z.W.); yuan040061@hrbeu.edu.cn (J.Y.); cocomomo@hrbeu.edu.cn (D.Y.); promotion5@foxmail.com (K.Z.); renjingfei@hrbeu.edu.cn (J.R.)

* Correspondence: cctime99@163.com

Abstract: The complex underwater environment poses significant challenges for unmanned underwater vehicles (UUVs), particularly in terms of communication constraints and the need for precise cooperative obstacle avoidance and trajectory tracking. Addressing these challenges solely through position information is crucial in this field. This study explores the intricate task of managing a group of UUVs as they navigate obstacles and follow a given trajectory, all based on position information. A new dynamic interactive topology framework utilizing sonar technology has been developed for the UUVs. This framework not only provides position information for the UUV swarm but also for the surrounding obstacles, enhancing situational awareness. Additionally, a bio-inspired cooperative control strategy designed for UUV swarms utilizing sonar interaction topology is introduced. This innovative method eliminates the need for velocity data from neighboring UUVs, instead relying solely on position information to achieve swarm cooperative control, obstacle avoidance, and trajectory adherence. The effectiveness of this method is validated through extensive simulations. The results show that the proposed method demonstrates improved sensitivity in obstacle detection, enabling faster trajectory tracking while maintaining a safer distance compared to traditional methods. Ultimately, this innovative strategy not only enhances operational efficiency but also enhances safety measures in UUV swarm operations.

Keywords: unmanned underwater vehicles; UUVs; cooperative control; bio-inspired; obstacle avoidance; sonar detection; tracking control

Citation: Wang, Z.; Wang, H.; Yuan, J.; Yu, D.; Zhang, K.; Ren, J. Bio-Inspired Cooperative Control Scheme of Obstacle Avoidance for UUV Swarm. *J. Mar. Sci. Eng.* **2024**, *12*, 489. https://doi.org/10.3390/jmse12030489

Academic Editor: Rafael Morales

Received: 9 February 2024
Revised: 6 March 2024
Accepted: 12 March 2024
Published: 14 March 2024

1. Introduction

In recent years, unmanned underwater vehicles (UUVs) have become an essential instrument in ocean engineering, serving a variety of purposes, such as monitoring, exploration, and surveillance, in particular in complex environments [1,2]. Due to the limited application scenarios of formation control technology [3], people are increasingly inclined to use UUV swarm technology to accomplish complex tasks in complex underwater environments. Nonetheless, coordinating the behavior of these swarms is challenging owing to potential swarm behavioral conflicts and chain reactions [4]. Bio-inspired collaborative control strategies have been gaining more recognition for managing conflicts within a group, avoiding collisions and obstacles, and carrying out tasks on the given trajectory in UUV swarm control [5].

The current collaborative control techniques mainly consist of centralized and distributed methods. However, when there are a large number of UUV clusters, the centralized distribution method is not feasible due to communication constraints in the underwater environment. In contrast, distributed control methods do not have a central control point, and information exchange is completed through mutual coordination between adjacent individuals, ultimately achieving the overall formation behavior. Due to the lack of a control center, distributed control systems are highly flexible and can dynamically change the structure of the control network. Distributed methods mainly consist of leader-following [6–8], virtual structure [9], artificial potential field [10] and consensus control [11,12].

There have been some studies on achieving trajectory tracking through distributed collaborative control. Article [13] proposes an experience-based distributed controller for an uncertain, high-order, nonlinear, multi-agent system to enhance the control performance and reduce the computational burden. Article [14] investigates a more practical constraint requirement that is dependent on the path parameter, rather than directly depending on the time variable. Article [15] presents a robust neuro-optimal control approach to enhance the robustness of a robot's tracking control under the influence of unknown nonlinear perturbations. Article [16] investigates the path-guided containment maneuvering of networked two-wheeled mobile robots with multiple virtual leaders moving along multiple parameterized paths. Paper [17] aims to address the cooperative path-following problem of autonomous surface vehicles (ASVs) over a wireless network with limited resources.

In terms of the impact of cluster interaction methods and the number of interactions on control results, the study in article [18] suggests that the swarm's adaptability improves when robots have fewer communication links. In paper [19], the authors investigate the platoon formation control problem for unmanned surface vehicles, accounting for modeling uncertainties and time-varying external disturbances along a given trajectory while maintaining a desired line-of-sight (LOS) range between each vehicle and its predecessor. Article [20] demonstrates various 3D collective behaviors, such as synchronization, dispersion/aggregation, dynamic circle formation, and search-and-capture, using a swarm of fish-inspired miniature underwater robots with implicit communication mediated by the production and sensing of blue light.

However, the above control methods have some limitations in solving the cooperative control problem of UUV clusters in underwater environments.

- Due to the complexity of the underwater environment, obstacle avoidance has become an important issue in the cooperative control of UUV clusters. However, the above articles have limited discussions on obstacle avoidance capabilities.
- In the underwater environment, the detection methods are limited, and sonar detection is a commonly used method. However, the above articles have limited research on sonar detection.
- Due to the harsh communication conditions underwater, obtaining velocity information from neighbors within the domain is extremely challenging.

Therefore, this study aims to address these limitations by proposing a novel approach that leverages only position information to achieve cooperative control among crowded UUV swarms, ensuring effective trajectory following while efficiently avoiding obstacles. Notably, this approach stands out for its ability to function without requiring velocity information. Through rigorous experimental validation and performance assessments, the efficacy and advantages of the proposed cooperative control approach are demonstrated in guiding crowded UUV swarms along a specified trajectory while efficiently maneuvering around obstacles.

The remaining sections are outlined as follows. Section 2 establishes the dynamic model of an UUV, presenting the problem statement. Section 3 analyzes sonar characteristics and proposes a dynamic interactive topology based on active and passive sonar detection. In Section 4, a bio-inspired collaborative control algorithm is proposed for the dynamic interactive topology. Section 5 validates the effectiveness of the proposed algorithm through simulation experiments on a constructed platform, specifically focusing on trajectory coordination, obstacle avoidance, and complex trajectory scenarios. Comparative experiments are conducted to verify the algorithm's efficiency in the presence of obstacles along the given trajectory. Finally, the paper concludes with a summary.

2. Problem Statement

2.1. The Dynamic Model of UUV

Taking into account the presence of n under-actuated UUVs. The motion description of each UUV is defined for the north-east-fixed reference frame and the body-fixed reference frame, as shown in Figure 1.

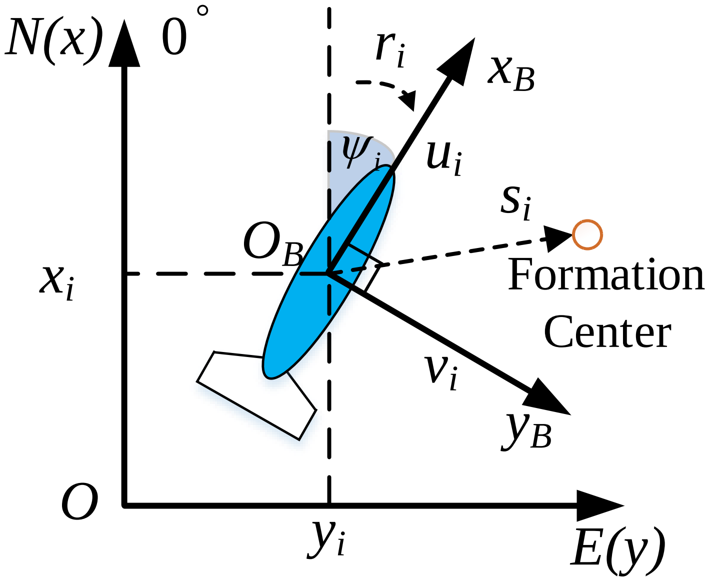

Figure 1. Global and body coordinate systems.

The north-east-fixed reference frame and body-fixed reference frame are shown in Figure 1. The 3 DOF control model of UUV is described as follows [21]:

$$\dot{\eta}_i = R(\psi_i)V_i \tag{1}$$

$$M_{RBi}\dot{V}_i + M_{Ai}\dot{V}_i + C_{RB}(V_i)V_i + C_A(V_i) + D(V_i)V_i = \tau_i \tag{2}$$

where $\eta_i = [x_i, y_i, \psi_i]^T$ represents the position and posture vector of the i-th UUV in the north-east-fixed reference frame. $R(\psi_i)$ is the transformation matrix from the north-east-fixed reference frame to the body-fixed reference frame. $V_i = [u_i, v_i, r_i]^T$ denotes the velocity vectors, including the surge, sway, and yaw, of the UUV in the body-fixed reference frame. The actuator input is represented by $\tau_i = [\tau_{ui}, 0, \tau_{ri}]^T$. τ_{ui} represents the thrust that affects the forward speed, and τ_{ri} represents the torque that affects the bow yaw angle.

$$\begin{aligned}
R(\psi_i) &= \begin{bmatrix} \cos\psi_i & -\sin\psi_i & 0 \\ \sin\psi_i & \cos\psi_i & 0 \\ 0 & 0 & 1 \end{bmatrix} \\
M_{RBi} &= \begin{bmatrix} m_i & 0 & 0 \\ 0 & m_i & m_i x_{Gi} \\ 0 & m_i x_{Gi} & I_{zi} \end{bmatrix} \\
M_{Ai} &= \begin{bmatrix} -X_{\dot{u}_i} & 0 & 0 \\ 0 & -Y_{\dot{v}_i} & -Y_{\dot{r}_i} \\ 0 & -Y_{\dot{r}_i} & -N_{\dot{r}_i} \end{bmatrix}
\end{aligned} \tag{3}$$

where $R(\psi_i)$ is the transformation matrix from the global coordinate system to the local coordinate system; M_{RBi} and M_{Ai} denote the inertia matrices of the rigid body and added mass, respectively; the mass of the i-th UUV is denoted as m_i.

$$
\begin{aligned}
C_{RB}(V_i) &= \begin{bmatrix} 0 & 0 & -m_i(x_{Gi}r_i + v_i) \\ 0 & 0 & m_i u_i \\ m_i(x_{Gi}r_i + v_i) & -m_i u_i & 0 \end{bmatrix} \\
C_A(V_i) &= \begin{bmatrix} 0 & 0 & Y_{\dot{v}_i} v_i + Y_{\dot{r}_i} r_i \\ 0 & 0 & -X_{\dot{u}_i} u_i \\ -Y_{\dot{v}_i} v_i - Y_{\dot{r}_i} r_i & X_{\dot{u}_i} u_i & 0 \end{bmatrix} \\
D_{li} &= \begin{bmatrix} X_{u_i} & 0 & 0 \\ 0 & Y_{v_i} & -Y_{r_i} \\ 0 & -N_{v_i} & N_{r_i} \end{bmatrix} \\
D_{nl}(V_i) &= \begin{bmatrix} X_{|u_i|u_i}|u_i| & 0 & 0 \\ 0 & Y_{|v_i|v_i}|v_i| & -Y_{|v_i|r}|v_i| \\ 0 & -N_{|r_i|v_i}|r_i| & N_{|r_i|r_i}|r_i| \end{bmatrix}
\end{aligned} \tag{4}
$$

where $C_{RB}(V_i)$ and $C_A(V_i)$ are Coriolis–centripetal matrices of rigid body and added mass, respectively; $D(V_i) = D_{li} + D_{nl}(V_i)$ is the system inertia matrix, Coriolis–centripetal matrix, and damping matrix.

Among these, the variables u_{ri} and v_{ri} represent the velocity components, while r_i represents the angular velocity of the UUV's motion. $X_{\dot{u}_i}$, X_{u_i}, $X_{|u_i|u_i}$, $Y_{\dot{v}_i}$, $Y_{\dot{r}_i}$, Y_{v_i}, Y_{r_i}, $Y_{|v_i|v_i}$, $N_{\dot{r}_i}$, $N_{\dot{r}_i}$, $N_{|r_i|r_i}$, and $Z_{\dot{w}}$ represent the ship's hydrodynamic forces and moments. The position of the center of gravity along the x-axis is denoted as x_{Gi}. I_Z is determined by the inertia matrix.

Subsequent research will be based on this UUV dynamic model to achieve the cooperative motion of UUVs through the control of τ_i.

2.2. Problem Statement

In the given scenario, as shown in Figure 2, the UUV swarm must track a given trajectory while avoiding obstacles and maintaining a safe distance from each other. Under the given trajectory, there are m obstacles and n UUVs. $\boldsymbol{O_i}$ represents the position of the i-th obstacle, and $\boldsymbol{x_i(t)}$ represents the position of the i-th UUV.

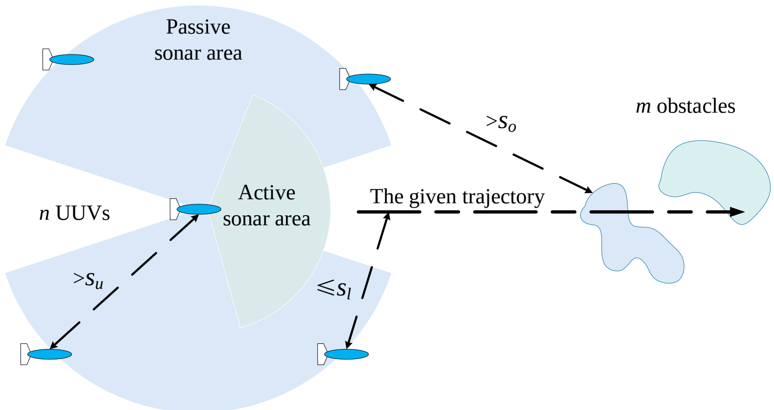

Figure 2. The problem statement of UUV swarm control.

The given trajectory can be considered as a virtual agent. At time t, the position of the trajectory is denoted as $\boldsymbol{l(t)}$:

$$
\boldsymbol{l}(t) = \begin{pmatrix} x_l(t) \\ y_l(t) \end{pmatrix} \tag{5}
$$

where $x_l(t)$ and $y_l(t)$ represent the position of the trajectory.

Then, at time t, the position of the i-th UUV $\boldsymbol{x_i(t)}$ can be expressed as

$$\boldsymbol{x_i(t)} = \begin{pmatrix} x_i(t) = x_{ri}(t) + x_l(t) \\ y_i(t) = y_{ri}(t) + y_l(t) \end{pmatrix} \tag{6}$$

where $x_i(t)$ and $y_i(t)$ represent the position of the i-th UUV, and $x_{ri}(t)$ and $y_{ri}(t)$ represent the relative position of the i-th UUV to the trajectory.

To avoid obstacles and maintain a safe distance from each other in the given trajectory, the UUV swarm must satisfy the following constraints:

$$\begin{cases} \|\boldsymbol{x_i(t)} - \boldsymbol{l(t)}\| \le s_l & \forall i \in \{1,2,\cdots,n\} \\ \|\boldsymbol{x_i(t)} - \boldsymbol{O_j}\| \ge s_o & \forall i,j \in \{1,2,\cdots,n\} \times \{1,2,\cdots,m\} \\ \|\boldsymbol{x_i(t)} - \boldsymbol{x_j(t)}\| \ge s_u & \forall i,j \in \{1,2,\cdots,n\} \times \{1,2,\cdots,n\} \end{cases} \tag{7}$$

where $\|\|$ represents the L_2 norm, and s_l, s_o, and s_u represent the maximum distance from the UUV to the trajectory, the safe distance from the UUV to the obstacle, and the safe distance within UUVs, respectively.

The objective of this study is to design a cooperative strategy that relies solely on position information to ensure that the UUVs avoid obstacles and maintain a safe distance while moving along the trajectory. The following are the key requirements of the cooperative strategy:

- All control strategies are based on position information and do not require velocity information.
- The cooperative motion of the swarm is achieved to ensure that the UUVs track the trajectory.
- The UUVs can avoid obstacles and maintain a safe distance when encountering obstacles.

3. Sonar Detection Interaction Topology

3.1. Interaction Topology

Interaction topology plays a key role in describing the collective behavior of biological groups [4,22,23]. This section discusses how to establish a dynamic interaction topology suitable for underwater sonar detection characteristics.

There are different types of local interactions studied in biology, including topological interactions, visual interactions, single-neighbor synergies, and multi-neighbor synergies [4,24,25]. Fish primarily respond to their single nearest neighbor [26], while pigeons adopt a hierarchical structure responding to their nearest neighbors [27]. These topologies simplify computational costs while enhancing robustness and sensitivity.

Early studies revealed that starlings mainly interact with their nearest 6–8 neighbors during flight [28]. This "topological interaction" forms a local interaction network that balances perception costs and group robustness [29,30]. By reducing the number of connections in the interaction topology, the efficiency of utilizing domain information can be effectively enhanced [31].

The traditional definition of an interaction neighborhood is one where an agent can interact equally with all others within a fixed sensing distance (Figure 3a). However, biological evidence indicates that a less complex topological interaction structure has a balance between perceived cost and group resilience (Figure 3b). Specifically, Figure 1 shows two models of interaction topology. In Figure 3, the green represents the individuals within the perception range, and the numbers are used to distinguish different individuals.

Sonar detection may also influence interaction topologies in biological groups. Sonar can detect the individuals within an agent's sensing range, potentially improving synchronization. Therefore, given the active and passive sonar characteristics of UUVs, we establish a dynamic interaction topology to acquire positional information within the field.

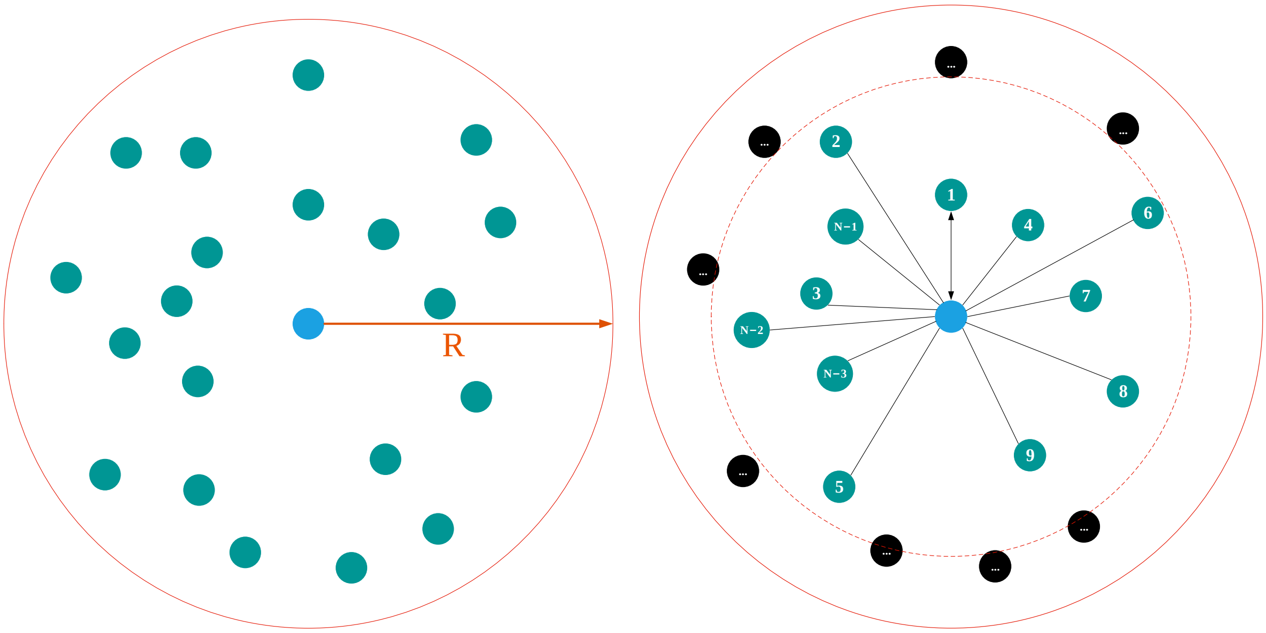

(**a**) The distance interaction (**b**) The topological interaction

Figure 3. (**a**) A metric-based neighborhood where all agents within a set radius can interact. This implies each agent processes an unlimited number of neighbors. (**b**) A topology-based neighborhood where agents selectively interact with a fixed number of closest neighbors.

3.2. Dynamic Interaction Models

3.2.1. Graphs Theory

It is practical to represent the interactions among agents' neighbors through an undirected or directed graph. In this model, each UUV is considered a node, and the interconnection structure within the UUV swarm can be characterized as a graph.

Assuming a graph $G(V_G, E, A)$ consisting of a node set $V_G = \{v_1, v_2, \ldots, v_n\}$ and an edge set $E \in V_G \times V_G$, where each edge is a pair of vertices(v_i, v_j) with $i \neq j$. If$(v_i, v_j) \in E$, then i and j are adjacent. $A = [a_{ij}] \in R^{n \times n}$ is the weighted adjacency matrix, where a_{ij} equals the corresponding weights if $(v_i, v_j) \notin E$, and 0 otherwise. The neighbor set of agent i is denoted as $N_i = \{v_j \in V_G | (v_i, v_j) \in E\}$. If $(v_i, v_j) \in E \Leftrightarrow (v_j, v_i) \in E$ is equivalent to$(v_i, v_j) \notin E$, G is an undirected graph; otherwise, it is a directed graph.

The utilization of mathematical tools from graph theory enables a clearer description of dynamic interaction models based on sonar detection.

3.2.2. Dynamic Interaction Models Based on Sonar Detection

Sonar detection plays a crucial role in swarm detection and spatial awareness. As shown in Figure 4, the dynamic interaction framework is established based on active and passive sonar detection. Active sonar involves emitting sound pulses and detecting their echoes, providing the emitting individual with precise spatial information about their surroundings. In contrast, passive sonar relies on the reception of sounds generated by other individuals, allowing for covert spatial awareness without the need for energy expenditure. Both modalities enable UUV to perceive their environment and neighbors, providing distance and directional information about detected objects. By analyzing and calculating distance and directional information, the position information of the neighbor set can be obtained.

To represent the interaction among agents, a graph, either undirected or directed, is employed to depict the interconnection topology. Due to the sonar detection, a directed graph is utilized to illustrate the interconnection topology of the UUV swarm, with each

UUV being treated as a node. This method proves to be advantageous in modeling the interaction among neighboring agents [21].

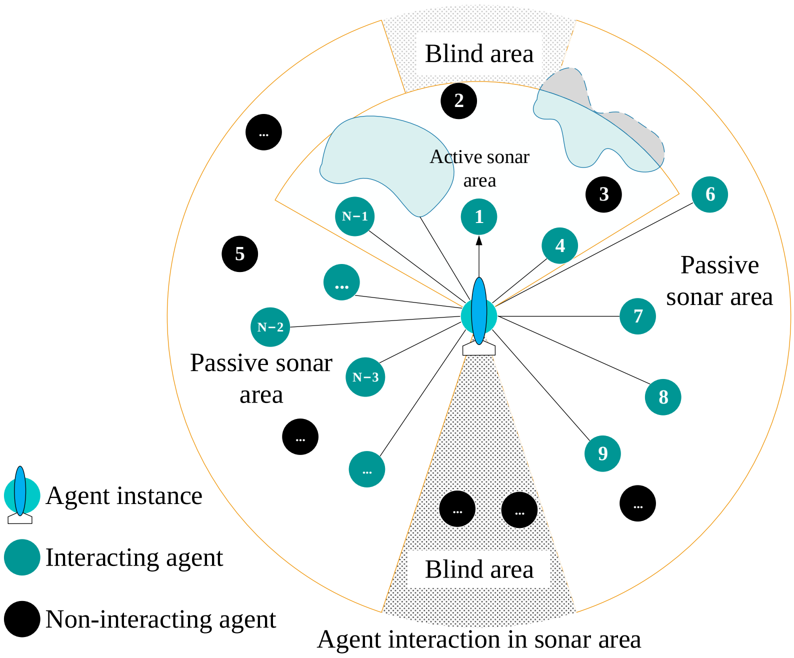

Figure 4. Dynamic interaction framework based on sonar.

Referring to the passive sonar of the i-th UUV, its detection length and angle range are defined as R_i and ϕ_i, respectively. The detection length and angle range of active sonar are defined as D_i and θ_i , respectively. For sonar detection, when objects overlap in the same direction, closer objects will overshadow farther ones, which is called sonar obscuration.

When ignoring sonar obscuration, the neighbor set within the passive sonar range of the i-th UUV can be expressed as

$$Q_i^p(t) = \{j|\psi_{ij} \in \phi_i \wedge \|\boldsymbol{x_i} - \boldsymbol{x_j}\| < R_i, \quad j \in \{1, \ldots, n\}, j \neq i\} \tag{8}$$

where ψ_{ij} is the heading from the j-th UUV to the i-th UUV. $\wedge$ is the logical AND operator.

The neighbor set within the active sonar range of the i-th UUV can be expressed as

$$Q_i^a(t) = \{j|\psi_{ij} \in \theta_i \wedge \|\boldsymbol{x_i} - \boldsymbol{x_j}\| < D_i, \quad j \in \{1, \ldots, n\}, j \neq i\} \tag{9}$$

Then, the neighbor set of i-th UUV in the passive and active sonar range can be expressed as

$$Q_i' = Q_i^p \cup Q_i^a \tag{10}$$

The obstacles can only be detected by the active sonar. If the number of obstacles is m, the obstacles within the active sonar range of the i-th UUV can be expressed as

$$O_i'(t) = \{j|\psi_{ij} \in \theta_i \wedge \|\boldsymbol{x_i(t)} - \boldsymbol{O_j}\| < D_i, \quad j \in \{1, ..., m\}\} \tag{11}$$

When considering the sonar obscuration [4], the heading θ_i is divided into k_a sector, as shown in Figure 5. Due to sonar obscuration, the active sonar detects the nearest individual in each sub-sector.

Then, the nearest individual in each sub-sector is chosen. The angle of the k-th sub-sector of the i-th UUV is calculated as follows:

$$\Theta_i^k = k\theta_i / k_a, m \in \{1, \ldots, k_a\} \tag{12}$$

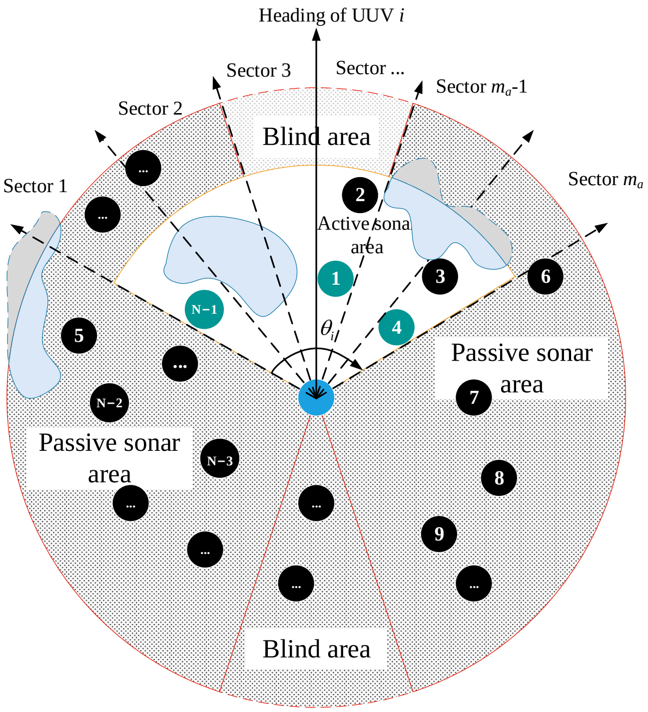

Figure 5. Dynamic interaction framework based on active sonar.

Then, the j-th neighbor in k-th sub-sector of the i-th UUV is shown as

$$M_i^k = \{j|\Theta_i^{k-1} \le \psi_{ij} - \psi_i \le \Theta_i^k\} \tag{13}$$

where ψ_i is the heading of the i-th UUV. Then, the nearest neighbors in each sub-sector $M_i^{k_a}(t)$ are chosen as

$$M_i^{k_a}(t) = \{j|j = \underset{j \in M_i^k}{argmin} \left\| \boldsymbol{x_i} - \boldsymbol{x_j} \right\|, k = 1, \ldots, k_a\} \tag{14}$$

So, considering the sonar obscuration, the neighbor set of i-th UUV can be expressed as

$$Q_i = \{j|j \in \left(Q_i' \cap M_i^{k_a}\right)\} \tag{15}$$

The nearest obstacle in each sub-sector $O_i^{k_a}(t)$ is chosen as

$$O_i^{k_a}(t) = \{j|j = \underset{j \in O_i'}{argmin} \left\| \boldsymbol{x_i} - \boldsymbol{O_j} \right\|, k = 1, \ldots, k_a\} \tag{16}$$

The obstacle set of the i-th UUV can be expressed as

$$O_i = \{j|j \in \left(O_i'(t) \cap O_i^{k_a}\right)\} \tag{17}$$

Therefore, we can gather information about the surrounding area, such as the presence of agents and obstacles, that aligns with the features of sonar detection.

4. Cooperative Control Method

The control methods for UUV swarm often rely on high-speed communication and precise velocity information [4,32], which can be challenging to maintain in underwater environments. Paper [23] presents a theoretical framework for designing and analyzing distributed flocking algorithms that rely on the position information of neighboring agents.

For obstacle avoidance, in this algorithm [23], obstacles are treated as moving agents. However, when the obstacle moves away, it is still considered an agent, which can disrupt the behavior of the agents and hinder the obstacle avoidance process. These constraints can hinder the effectiveness of UUV cluster control, particularly in scenarios with limited communication conditions.

In nature, biological collectives can exhibit rather complex functionalities through simple self-organizing behaviors [33]. Based on this understanding, a bio-inspired control strategy is proposed.

Through the use of sonar-based interaction topology, individuals within a cluster can utilize this model to obtain information about their current neighborhoods and obstacles. Leveraging the characteristics of active and passive sonar, UUVs can employ passive sonar for cluster aggregation and collision avoidance, while active sonar can be used for obstacle avoidance. This approach effectively reduces the demands on UUV cluster coordination for complex tasks, ultimately lowering the overall computational and communication requirements.

Considering the three constraints (7) in the problem description, inspired by the paper [23] and biological collectives, this paper designs a bio-inspired, position-based, cooperative control strategy to satisfy the three constraints under the sonar interaction topology.

Since the cooperative control strategy needs to satisfy the three constraints of path tracking, obstacle avoidance, and maintaining a safe distance, the designed control strategy is a combination of three control strategies. The excepted variable $\boldsymbol{\tau_i}(t)$ of the i-th UUV can be expressed as

$$\boldsymbol{\tau_i}(t) = \boldsymbol{\tau_i^l}(t) + \boldsymbol{\tau_i^n}(t) + \boldsymbol{\tau_i^o}(t) \tag{18}$$

$\boldsymbol{\tau_i^l}(t)$ represents the trajectory coordination between the given trajectory and the position of the i-th UUV at time t. The UUV swarm tracks the given trajectory through $\boldsymbol{\tau_i^l}(t)$.

$$\boldsymbol{\tau_i^l}(t) = \xi_l(\boldsymbol{l(t)} - \boldsymbol{x_i(t)}) \tag{19}$$

where parameter ξ_l is used to adjust the strength of the UUV towards the trajectory point. By adjusting the size of the parameter ξ_l, the UUV can be attracted to the trajectory point, allowing the UUV to move along the given trajectory. Moreover, by setting the change in ξ_l concerning time, the UUV can have different attractions to the trajectory point at different times, thereby achieving different tracking accuracies of the trajectory point at different times.

$\boldsymbol{\tau_i^n}(t)$ is the coordination term between the agent and its neighbors obtained through the dynamic interaction topology. By designing $\boldsymbol{\tau_i^n}(t)$, the cooperative motion between UUVs can be achieved, ensuring that UUVs can achieve adaptive aggregation and maintain a safe distance.

$$\boldsymbol{\tau_i^n}(t) = \sum_{j \in Q_i} \xi_n(\boldsymbol{x_i}(t) - \boldsymbol{x_j}(t))\left(\exp\left(\frac{\delta_n}{\|\boldsymbol{x_i}(t) - \boldsymbol{x_j}(t)\|}\right) - \exp(1)\right) \tag{20}$$

where Q_i is the set of neighboring UUVs obtained by sonar detection interaction topology. ξ_n is the coordination weight, used to adjust the proportion of the three forces of swarm, trajectory tracking, and obstacle avoidance. By adjusting the size of ξ_n, the cluster can respond more sensitively to one of the forces. δ_n is the safe distance adjustment parameter. By adjusting the size of δ_n, the range of repulsion and attraction between two UUVs can be changed, so that the UUVs repel each other at close range and attract each other at long range.

$\boldsymbol{\tau_i^o}(t)$ is the coordination term between the agent and the obstacle in active sonar.

$$\boldsymbol{\tau_i^o}(t) = \sum_{j \in O_i} \xi_o \exp\left(\frac{\delta_o}{\|\boldsymbol{x_i}(t) - \boldsymbol{O_j}\|}\right)(\boldsymbol{x_i}(t) - \boldsymbol{O_j}) \tag{21}$$

where ξ_o is the obstacle avoidance weight, used to adjust the proportion of the obstacle avoidance force. By adjusting the size of ξ_o, the cluster can respond more sensitively to the obstacle avoidance force. δ_o is the distance adjustment parameter. By adjusting the size of δ_o, the cluster can respond more sensitively to the distance of the obstacle.

The expected force $\boldsymbol{\tau_i}(t)$ of the UUV can be obtained. By decomposing the velocity direction and the vertical direction of $\boldsymbol{\tau_i}(t)$, the τ_{ui} and τ_{ri} in Equation (2) can be obtained as follows

$$\begin{aligned} \tau_{ui} &= \boldsymbol{\tau_i}(t) \cdot (\cos(\psi_i), \sin(\psi_i)) \\ \tau_{ri} &= \boldsymbol{\tau_i}(t) \cdot (-\sin(\psi_i), \cos(\psi_i)) \end{aligned} \tag{22}$$

where τ_{ui} is the force in the direction of the UUV velocity and τ_{ri} is the torque. $\cdot$ is the dot product of two vectors.

Define t_r as the simulation step; then, the velocity and position of the UUV can be updated using the fourth-order Runge–Kutta method [34]. Define the differential equation of Equation (2) as $\dot{V}_i = f_\tau(\boldsymbol{V_i}, \boldsymbol{\tau_i})$, and the differential equation of Equation (1) as $\dot{\eta}_i = f_V(\boldsymbol{\eta_i}, \boldsymbol{V_i})$. If at time t, the position and attitude vector of the i-th UUV is $\boldsymbol{\eta_i(t)}$ and the velocity and angular velocity vector is $\boldsymbol{V_i(t)}$, then at time $t + t_r$, the velocity of the UUV is

$$\begin{cases} \boldsymbol{V_i}(t+t_r) = \boldsymbol{V_i}(t) + t_r/6(\boldsymbol{k_1} + 2\boldsymbol{k_2} + 2\boldsymbol{k_3} + \boldsymbol{k_4}) \\ \boldsymbol{k_1} = f_\tau(\boldsymbol{V_i}(t), \boldsymbol{\tau_i}) \\ \boldsymbol{k_2} = f_\tau(\boldsymbol{V_i}(t) + \boldsymbol{k_1} t_r/2, \boldsymbol{\tau_i}) \\ \boldsymbol{k_3} = f_\tau(\boldsymbol{V_i}(t) + \boldsymbol{k_2} t_r/2, \boldsymbol{\tau_i}) \\ \boldsymbol{k_4} = f_\tau(\boldsymbol{V_i}(t) + \boldsymbol{k_3} t_r, \boldsymbol{\tau_i}) \end{cases} \tag{23}$$

Then, the position of the UUV is

$$\begin{cases} \boldsymbol{\eta_i}(t+t_r) = \boldsymbol{\eta_i}(t) + t_r/6(\boldsymbol{k_1} + 2\boldsymbol{k_2} + 2\boldsymbol{k_3} + \boldsymbol{k_4}) \\ \boldsymbol{k_1} = f_V(\boldsymbol{\eta_i}(t), \boldsymbol{V_i}(t)) \\ \boldsymbol{k_2} = f_V(\boldsymbol{\eta_i}(t) + \boldsymbol{k_1} t_r/2, \boldsymbol{V_i}(t + t_r/2)) \\ \boldsymbol{k_3} = f_V(\boldsymbol{\eta_i}(t) + \boldsymbol{k_2} t_r/2, \boldsymbol{V_i}(t + t_r/2)) \\ \boldsymbol{k_4} = f_V(\boldsymbol{\eta_i}(t) + \boldsymbol{k_3} t_r, \boldsymbol{V_i}(t)) \end{cases} \tag{24}$$

Thus, the high-precision position and attitude information of the UUV can be obtained. Next, the cooperative control strategy proposed in this paper will be verified by simulation.

5. Simulation Results

To assess the practicality and efficacy of the proposed bio-inspired cooperative control scheme, a simulation platform for UUVs was constructed using Unity, as illustrated in Figure 6.

The control scheme uses Unity to build the marine environment, which contains the UUV dynamics model, Doppler velocity logs, positioning transponders, and sonar for detection. The collaborative control method is developed in Python and interfaces with the simulation platform to validate the proposed method. In this simulation platform, depicted in Figure 6, the movement of UUVs in the ocean can be replicated. The UUV swarm gathers data using Doppler velocity logs, positioning transponders, and sonar for detection. This information is then processed through an interactive topology to determine obstacle and UUV positions within the nearby area. Subsequently, the UUV calculates its anticipated force using collaborative control techniques and tests the proposed method using the simulation platform.

The parameters of the proposed method are set as follows in Table 1.

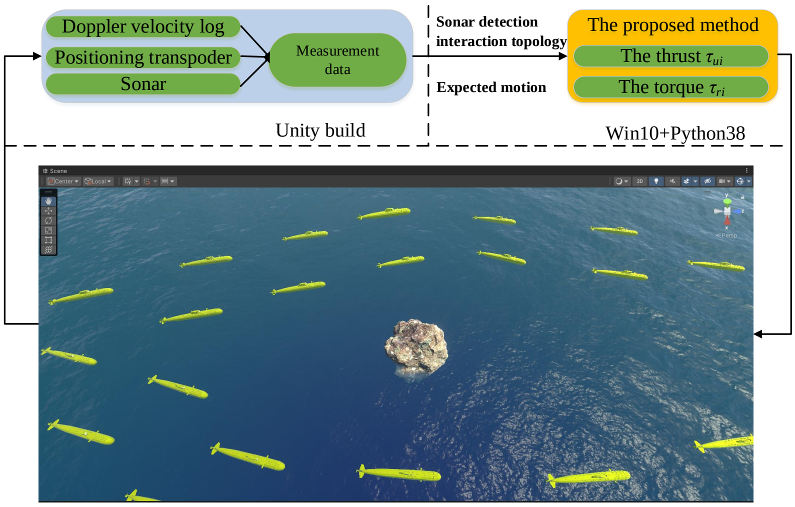

Figure 6. Simulation configuration and experimental platform.

Table 1. Parameters of the proposed method.

Parameter	Value	Parameter	Value
ξ_l	30	t_r	0.1 s
ξ_n	0.8	ϕ_i	120°
δ_n	60	θ_i	120°
ξ_o	8	R_i	500 m
δ_o	80	D_i	100 m

5.1. The Effectiveness of Trajectory Tracking without Obstacles

To verify the effectiveness of the proposed method in trajectory tracking, this paper conducted a trajectory tracking simulation of the UUV swarm on the simulation platform. In the simulation, the UUVs were divided into two groups, as depicted in Figure 7a, and placed in a rectangular area of 100×200. The initial velocities of the UUVs were randomly assigned between 0 and 4 m/s.

The trajectory is a line from [180, 180] m to [800, 100] m, then to [500, 600] m, and finally to [1000, 1000] m. The expected speed of this trajectory is 4 m/s. The UUV swarm is required to track the given trajectory. No adjustment of the above control method is required, and the UUV swarm can track the given trajectory. The simulation results are presented as shown below.

The initial pattern of the UUV swarm is shown in Figure 7a, where the circles represent the positions of individual UUVs and the arrows represent the velocity vectors of UUVs. The length of the arrow represents the velocity magnitude of the UUV, and the direction of the arrow represents the heading direction of the UUV. Figure 7b shows the position and pose of the UUV swarm when it reaches the end of the trajectory. It can be seen that the UUV swarm forms a stable formation, with stable distances between each UUV. The UUV swarm has transformed from a chaotic state to an orderly state through the proposed method.

The motion trajectory of the UUV swarm under the given trajectory is shown in Figure 8. As shown in Figure 8a, under the action of the control law in the given trajectory, UUV swarm individuals gradually gather in groups from the initial random state distribution, and then the swarm moves along the given trajectory. And, when the swarm turns at the position [800, 100], some UUVs continuously expand towards the edge of the swarm to ensure internal collision avoidance. By intuitively looking at Figure 8b, it can be seen that the center of the UUV swarm coincides with the given trajectory.

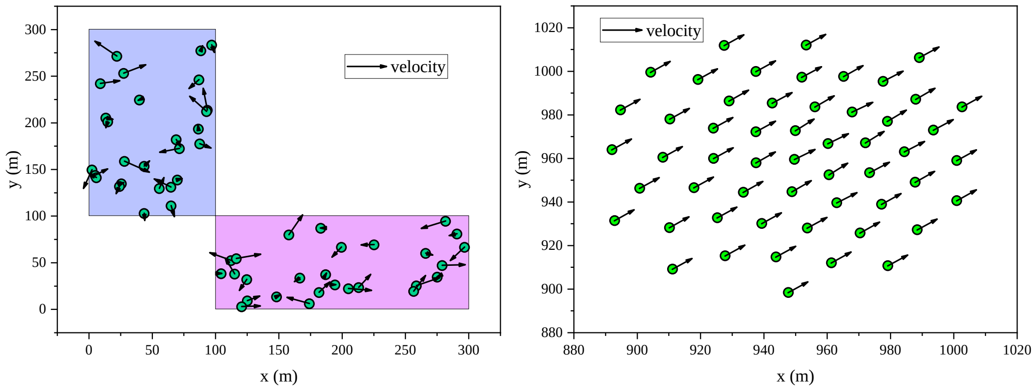

(**a**) Initial pattern of the UUV swarm. (**b**) Final pattern of UUV swarm.

Figure 7. Comparison of the initial and final states of the UUV swarm.

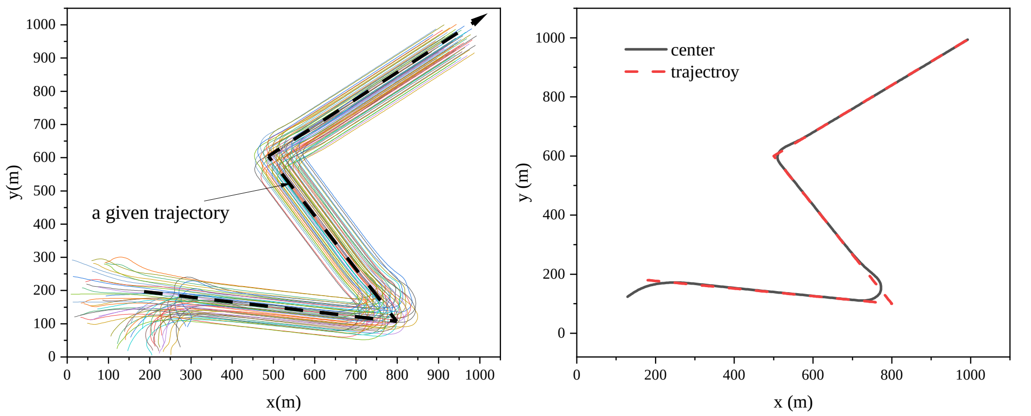

(**a**) The motion trajectory of the UUV swarm. (**b**) The center of the swarm and the given trajectory.

Figure 8. Route tracking results of the UUV swarm.

Next, the effect of trajectory tracking and the cooperative effect were further analyzed. The heading of the UUV swarm and the deviation between the center of the swarm and the given trajectory were statistically analyzed, and the graphs shown in Figure 9a,b were created.

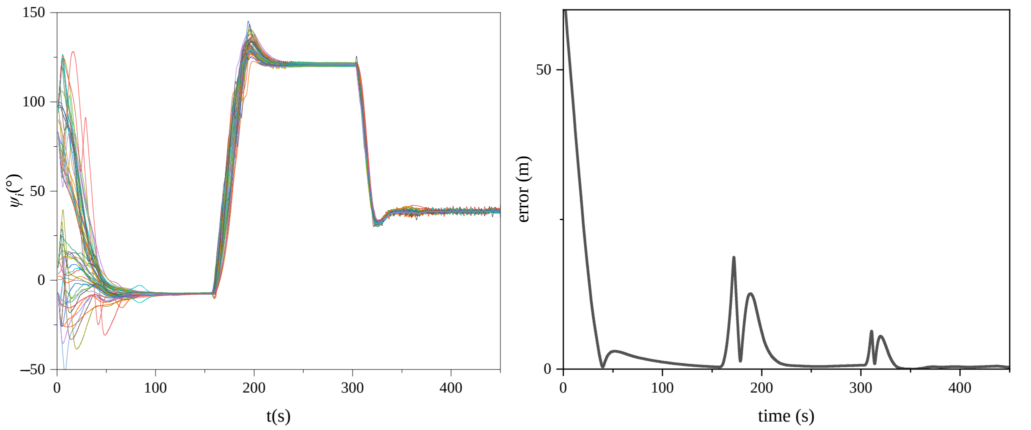

(**a**) The heading of UUV swarm. (**b**) Error between swarm center and trajectory.

Figure 9. The heading of UUV swarm and error between swarm center and given trajectory.

As shown in Figure 9a, the UUV swarm gradually tends to be consistent under the proposed method, and the heading of the UUV swarm changes significantly near the turning point of the given trajectory. This is because the UUV swarm needs to be reorganized near the turning point of the given trajectory. As shown in Figure 9b, the deviation of the center of the UUV swarm under a stable trajectory will gradually decrease. When a turning point occurs, the deviation of the center of the UUV swarm will increase because of reorganization, but after the turning point, the deviation of the center of the UUV swarm will gradually decrease. This indicates that the UUV swarm can effectively track the given trajectory.

Recording the maximum and minimum distances between UUVs can reveal the stability of the UUV swarm under the given trajectory.

The maximum and minimum distances between UUVs in the swarm are shown in Figure 10. As shown in the figure, the maximum and minimum distances between UUVs in the swarm under the given trajectory can stabilize within a certain range. Near the turning point of the given trajectory, the change in the minimum distance is not significant, and the minimum distance between UUVs will not be less than 10.03 m. The average minimum distance is 12.29 m. This indicates that, under the given trajectory, the UUV swarm can maintain a stable safe distance and has a certain stability.

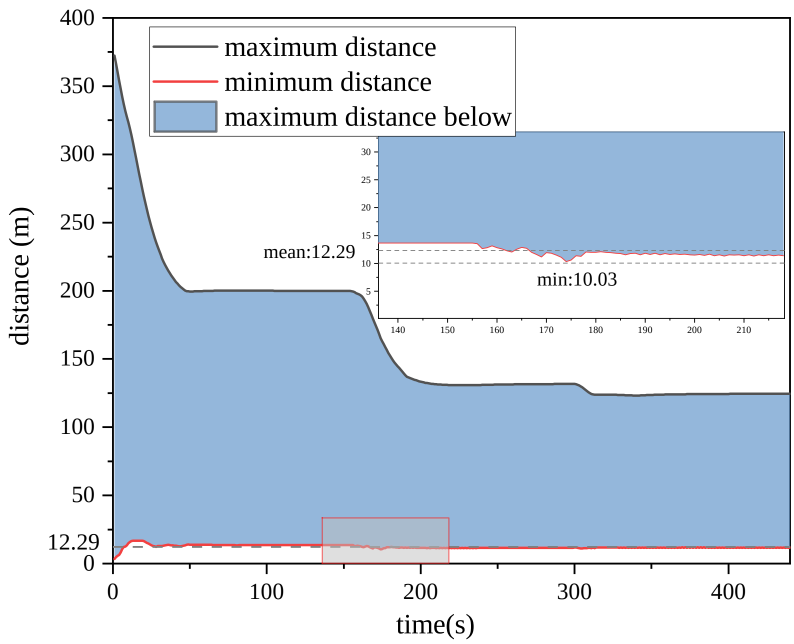

Figure 10. The max–min distances between UUVs.

The UUV swarm can effectively track the given trajectory and maintain a stable formation, demonstrating the effectiveness of the proposed control law in achieving cooperative control and trajectory tracking.

5.2. The Effectiveness of Trajectory Tracking within Obstacle Avoidance

In this section, the obstacle avoidance capability of the proposed method in the presence of single and multiple obstacles along a given trajectory is verified.

5.2.1. Single Obstacle Avoidance

First, the trajectory tracking effect of the proposed method under a single obstacle is verified. The trajectory is a straight line from [150, 150] m to [600, 600] m. The number of UUVs was set to 54, and an obstacle was added to the given trajectory. The obstacle is located at [350, 350] and is a circular obstacle with a diameter of approximately 50 m. Under the control method proposed in this paper, the UUV swarm moves along the given trajectory, and the results are shown in Figure 11.

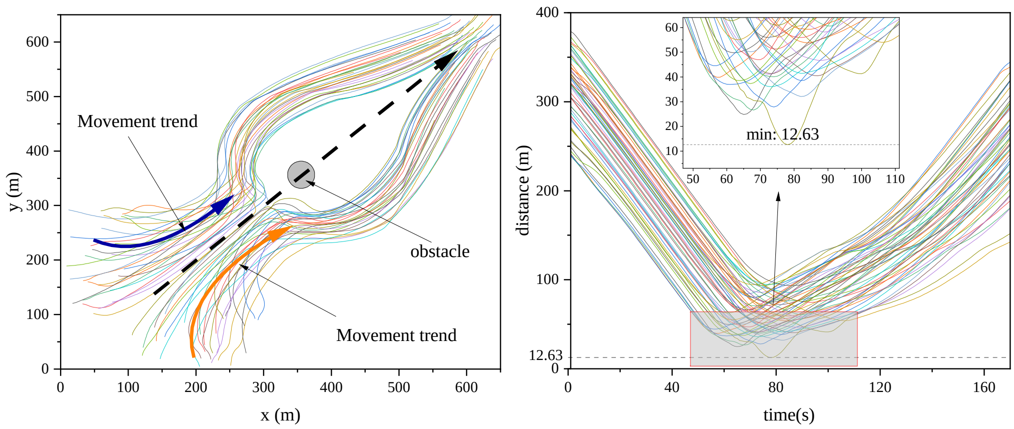

(**a**) Route tracking within obstacle simulation. (**b**) Min distance from UUV to obstacle.

Figure 11. Route tracking within obstacle simulation.

Figure 11a illustrates the movement trajectory of the UUV swarm when traversing a trajectory containing obstacles. At the initial state, the UUV swarm is affected by both the cooperative control and the target trajectory. The UUV swarm in the two areas gradually gathers along the direction of the blue and orange arrows. When it approaches the obstacle, it is affected by the repulsion force of the obstacle, and begins to disperse and avoid the obstacle. After the UUV swarm passes through the obstacle, it is affected by the attraction force of the target trajectory, and re-gathers. During the crossing process, the minimum distance between the UUV and the obstacle changes with time, as shown in Figure 11b.

The minimum distance between UUVs and the obstacle during the traversal process is shown in Figure 11b. It can be observed that the distance between UUVs and the obstacle is always greater than 12.63 m.

The obstacle avoidance effect of the proposed cooperative strategy mainly depends on the adjustment of ξ_o and δ_o. ξ_o is the obstacle avoidance weight, and by adjusting the size of ξ_o, the cluster can respond more sensitively to the obstacle avoidance force. δ_o is the distance adjustment parameter, and by adjusting the size of δ_o, the UUV can always maintain a certain safe distance.

When ξ_o is too small, as shown in Figure 12a, the UUV swarm cannot complete the obstacle avoidance. Due to the small ξ_o, the UUV swarm is not sensitive enough to the obstacle avoidance force, resulting in the UUV swarm being unable to avoid obstacles in time. When ξ_o is too large, the UUV swarm will exhibit excessive obstacle avoidance, as shown in Figure 12b. During the obstacle avoidance process, the UUV swarm will exhibit excessive obstacle avoidance, resulting in the motion trajectory of the UUV swarm not being smooth enough.

δ_o is the distance adjustment parameter, and by adjusting the size of δ_o, the UUV can always maintain a certain safe distance. When δ_o is too small, as shown in Figure 13a, the UUV swarm will be too close to the obstacle, which may cause a collision. When δ_o is too large, as shown in Figure 13b, although the UUV swarm can complete the obstacle avoidance, it will waste too much energy for obstacle avoidance. Therefore, different task requirements need to adjust δ_o.

It can be seen that for simple, single obstacle avoidance, the proposed method can be used for tasks with different obstacle avoidance requirements. By adjusting the size of ξ_o and δ_o, the UUV swarm can complete obstacle avoidance under the given trajectory and maintain a certain safe distance. This verifies the obstacle avoidance effect of the proposed method under simple obstacles.

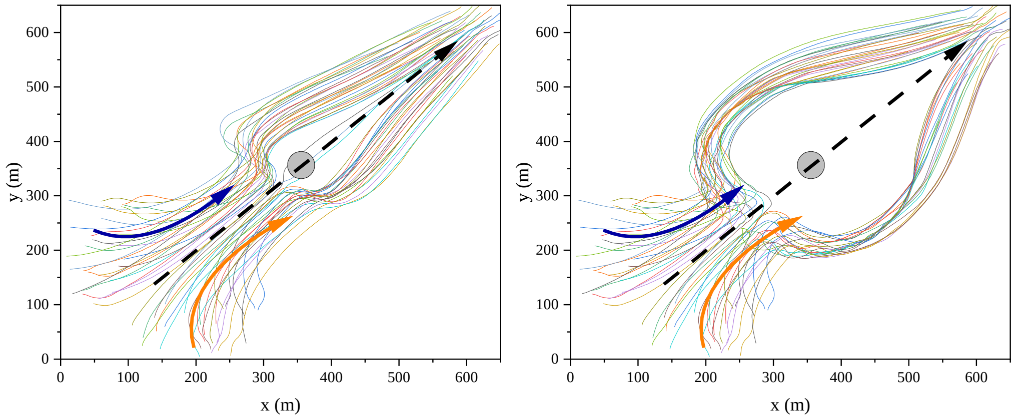

(**a**) $\xi_o = 2$, $\delta_o = 80$ (**b**) $\xi_o = 20$, $\delta_o = 80$

Figure 12. The effect of ξ_o on obstacle avoidance.

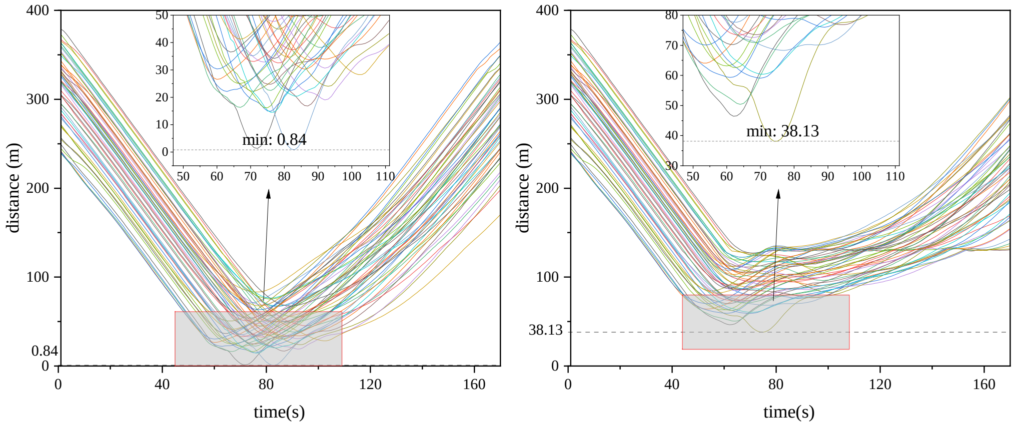

(**a**) $\delta_o = 50$, $\xi_o = 8$ (**b**) $\delta_o = 130$, $\xi_o = 8$

Figure 13. The effect of ξ_o on obstacle avoidance.

5.2.2. Multiple Obstacles Avoidance

This section will verify the complex trajectory tracking effect of the proposed method under multiple obstacles. To validate the effectiveness of the proposed control method in executing complex trajectories with multiple obstacles, the following simulation scenario is designed.

As shown in Figure 14, the trajectory is a line from [200, 200] m to [800, 100] m, then to [500, 600] m, and finally to [1000, 1000] m. Four obstacles are located at [600, 100] m, [400, 200] m, [700, 850] m, and [700, 700] m, and all of them are circular. The diameter of the obstacles is 50 m. The UUV swarm is tasked with trajectory tracking, and the results are shown in the figure.

Figure 15 shows the variation in the minimum distance between the UUV swarm and each obstacle during the trajectory tracking task. As can be seen from the figure, even when traversing a complex trajectory containing multiple obstacles, the proposed method can still ensure a safe distance of more than 6.34 m between the UUVs and the obstacles, thus verifying the effectiveness of the proposed method.

The traversal tracking task was completed in 527 s through the cooperative control method designed in this paper. As shown in Figure 14, the UUV cluster can navigate according to the given trajectory and perform timely obstacle avoidance and intra-cluster collision avoidance when encountering obstacles, demonstrating high intelligence and execution efficiency.

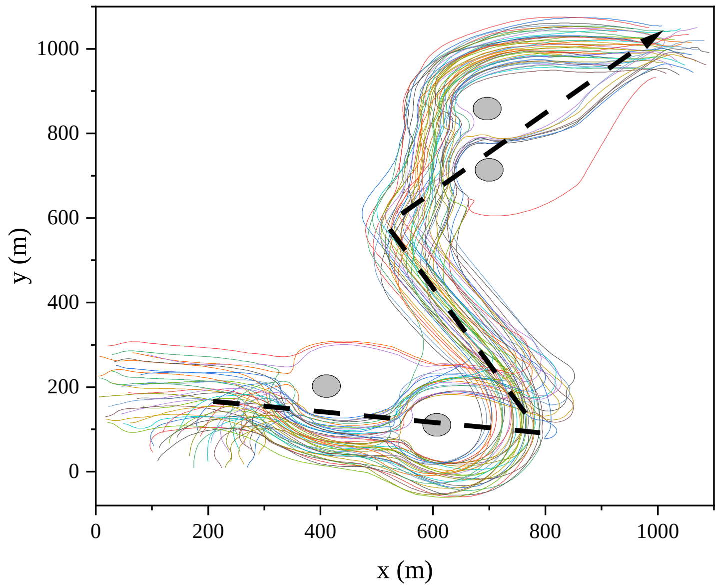

Figure 14. The minimum distance from UUV to obstacle.

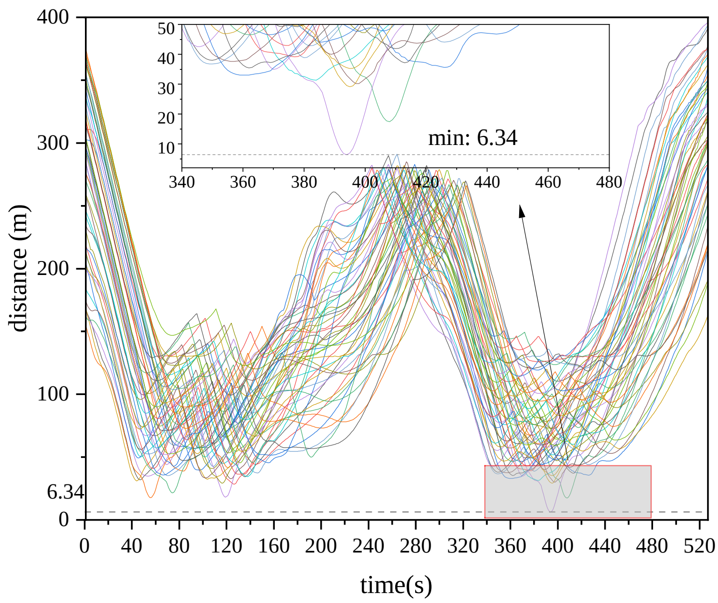

Figure 15. The minimum distance from UUVs to obstacles.

It can be concluded that, under the control method proposed in this paper, the UUV swarm can automatically split into groups for obstacle avoidance when encountering obstacles, and then regroup under the attraction of the trajectory and the swarm. The distance between UUVs is always maintained above a safe distance. The above analysis verifies that the control method proposed can achieve trajectory tracking with obstacles on a given trajectory by relying only on position information without the need for speed of the neighbors, and realizes UUV swarm cooperative control, collision avoidance, and obstacle avoidance control.

5.3. Comparison with Existing Methods

The greatest advantage of this control method is that it does not require the velocity information of neighbors, and can achieve swarm cooperative control, obstacle avoidance, and trajectory tracking with only positional information.

The self-organized fission/fusion method (SFF) [33] method and single-informed-based distributed consensus (SDC) [19] method were selected for obstacle avoidance simulation verification. The SFF method predicts the future state of neighbors by utilizing historical information and realizes the split and aggregation of the swarm by designing the clustering and splitting terms. The SDC method proposes an adaptive formation control that ensures a closed-loop system's internal stability with guaranteed prescribed performance. Both the SFF method and the SDC method adopted the velocity coordination term. To compare the advantages and disadvantages of the proposed method with existing methods, the task execution time consumption and the safety distance of the proposed method, the SFF method, and the SDC method were compared. The trajectory tracking simulation results under a single obstacle were selected for comparison. After incorporating obstacle avoidance, the time consumption of the three methods is presented in Table 2.

Table 2. Comparison of time cost of three methods.

Method	Task Execution Time (s)	Minimum Distance between UUV and Obstacle (m)
SDC	206	4.2
SFF	208	3.7
Proposed	205	10.48

Table 2 shows that the proposed method in this paper has higher efficiency in trajectory tracking with obstacles, and can complete the tracking in a shorter time and with a larger safety distance.

To analyze the differences in simulation results between the proposed control method and the two methods mentioned above, it is noted that the proposed method does not use a velocity coordination term to control the swarm. Instead, it relies solely on positional information to perform cooperative control, obstacle avoidance, and trajectory tracking. Therefore, the proposed method is more sensitive to the presence of obstacles and has a larger safety distance compared to the other two methods. Moreover, it shows better execution performance in tracking the given trajectory.

6. Conclusions

This paper addresses the problem of controlling a swarm of UUVs with obstacles in a given trajectory based on position information. A dynamic interactive topology framework based on sonar is designed for UUVs, which provides the position information of both the swarm and obstacles. Then, a bio-inspired cooperative control method for UUV swarm based on sonar interaction topology is proposed. The method does not require the velocity information of neighbors and only needs position information to achieve swarm cooperative control, obstacle avoidance, and trajectory tracking. The effectiveness of the proposed method is verified through simulation experiments. The results show that the UUV swarm can effectively track the given trajectory and maintain a stable formation, demonstrating the effectiveness of the proposed control method in achieving cooperative control and trajectory tracking. The proposed method is more sensitive to the presence of obstacles and can complete the tracking in a shorter time and with a larger safety distance compared to existing methods.

The proposed method only relies on position information, greatly reducing the communication burden of the UUV swarm, and enabling the UUV swarm to achieve complex trajectory tracking based solely on the position information obtained by sonar detection, demonstrating high intelligence and execution efficiency. This method holds promising applications in various scenarios, such as underwater infrastructure inspection, environmental monitoring, search-and-rescue operations, and oceanographic research.

In future work, we will focus on the following aspects: (1) a theoretical stability analysis of the method will be conducted; (2) the potential consequences on the cluster in the event of a sensor failure will be studied; (3) the proposed method will be further verified in a real underwater environment.

Author Contributions: Conceptualization, H.W.; methodology, Z.W.; software, Z.W. and J.Y.; validation, Z.W. and D.Y.; formal analysis, Z.W. and D.Y.; investigation, Z.W. and K.Z.; resources, Z.W., J.Y., D.Y. and K.Z.; data curation, Z.W.; writing—original draft, Z.W.; writing—review and editing, H.W., J.Y. and J.R.; visualization, Z.W., K.Z. and J.R.; project administration, H.W.; funding acquisition, H.W. All authors have read and agreed to the published version of the manuscript.

Funding: This research work was supported by the National Science and Technology Innovation Special Zone Project (21-163-05-ZT-002-005-03), the National Key Laboratory of Underwater Robot Technology Fund (No. JCKYS2022SXJQR-09), and a special program to guide high-level scientific research (No. 3072022QBZ0403).

Institutional Review Board Statement: Not applicable.

Informed Consent Statement: Not applicable.

Data Availability Statement: Data are contained within the article.

Conflicts of Interest: The authors declare no conflict of interest.

References

1. Liang, H.; Qiang, N. Distributed Cooperative Control Based on Dynamic Following Interaction Mechanism for UUV Swarm. In Proceedings of the 2020 39th Chinese Control Conference (CCC), Shenyang, China, 27–29 July 2020; pp. 5092–5097.
2. Wu, Y.; Low, K.H.; Lv, C. Cooperative Path Planning for Heterogeneous Unmanned Vehicles in a Search-and-Track Mission Aiming at an Underwater Target. *IEEE Trans. Veh. Technol.* **2020**, *69*, 6782–6787. [CrossRef]
3. Ingrand, F.; Ghallab, M. Deliberation for Autonomous Robots: A Survey. *Artif. Intell.* **2017**, *247*, 10–44. [CrossRef]
4. Liang, H.; Fu, Y.; Gao, J. Bio-Inspired Self-Organized Cooperative Control Consensus for Crowded UUV Swarm Based on Adaptive Dynamic Interaction Topology. *Appl. Intell.* **2021**, *51*, 4664–4681. [CrossRef]
5. Liang, H.; Fu, Y.; Kang, F.; Gao, J.; Qiang, N. A Behavior-Driven Coordination Control Framework for Target Hunting by UUV Intelligent Swarm. *IEEE Access* **2020**, *8*, 4838–4859. [CrossRef]
6. Wang, J.; Wang, C.; Wei, Y.; Zhang, C. Neuroadaptive Sliding Mode Formation Control of Autonomous Underwater Vehicles With Uncertain Dynamics. *IEEE Syst. J.* **2020**, *14*, 3325–3333. [CrossRef]
7. Yan, Z.; Liu, Y.; Yu, C.; Zhou, J. Leader-following coordination of multiple UUVs formation under two independent topologies and time-varying delays. *J. Cent. South Univ.* **2017**, *24*, 382–393. [CrossRef]
8. Yan, Z.; Xu, D.; Chen, T.; Zhang, W.; Liu, Y. Leader-Follower Formation Control of UUVs with Model Uncertainties, Current Disturbances, and Unstable Communication. *Sensors* **2018**, *18*, 662. [CrossRef] [PubMed]
9. Li, J.; Guo, H.; Zhang, H.; Yan, Z. Double-Loop Structure Integral Sliding Mode Control for UUV Trajectory Tracking. *IEEE Access* **2019**, *7*, 101620–101632. [CrossRef]
10. Sahu, B.K.; Subudhi, B. Flocking Control of Multiple AUVs Based on Fuzzy Potential Functions. *IEEE Trans. Fuzzy Syst.* **2018**, *26*, 2539–2551. [CrossRef]
11. Fan, J.; Zhao, L. Distributed Adaptive Consensus Tracking Control for Multiple AUVs with State Constraints. In *Proceedings of 2020 Chinese Intelligent Systems Conference*; Jia, Y., Zhang, W., Fu, Y., Eds.; Springer: Singapore, 2021; pp. 317–325.
12. Chen, W.; Hua, S.; Zhang, H. Consensus-Based Distributed Cooperative Learning From Closed-Loop Neural Control Systems. *IEEE Trans. Neural Netw. Learn. Syst.* **2015**, *26*, 331–345. [CrossRef]
13. Dai, S.-L.; He, S.; Ma, Y.; Yuan, C. Distributed Cooperative Learning Control of Uncertain Multiagent Systems With Prescribed Performance and Preserved Connectivity. *IEEE Trans. Neural Netw. Learn. Syst.* **2021**, *32*, 3217–3229. [CrossRef] [PubMed]
14. Jin, X.; Dai, S.-L.; Liang, J.; Guo, D. Adaptive Path-Following Control of An Autonomous Vehicle with Path-Dependent Constraint Requirements. In Proceedings of the 2021 60th IEEE Conference on Decision and Control (CDC), Austin, TX, USA, 14–17 December 2021; pp. 5753–5758.
15. Kong, L.; He, W.; Yang, C.; Sun, C. Robust Neurooptimal Control for a Robot via Adaptive Dynamic Programming. *IEEE Trans. On Neural Netw. Learn. Syst.* **2021**, *32*, 2584–2594. [CrossRef] [PubMed]
16. Gu, N.; Peng, Z.; Wang, D.; Zhang, F. Path-Guided Containment Maneuvering of Mobile Robots: Theory and Experiments. *IEEE Trans. Ind. Electron.* **2021**, *68*, 7178–7187. [CrossRef]
17. Lv, M.; Peng, Z.; Wang, D.; Han, Q.-L. Event-Triggered Cooperative Path Following of Autonomous Surface Vehicles Over Wireless Network With Experiment Results. *IEEE Trans. Ind. Electron.* **2022**, *69*, 11479–11489. [CrossRef]
18. Talamali, M.S.; Saha, A.; Marshall, J.A.R.; Reina, A. When Less Is More: Robot Swarms Adapt Better to Changes with Constrained Communication. *Sci. Robot.* **2021**, *6*, eabf1416. [CrossRef] [PubMed]
19. Dai, S.-L.; He, S.; Lin, H.; Wang, C. Platoon Formation Control With Prescribed Performance Guarantees for USVs. *IEEE Trans. Ind. Electron.* **2018**, *65*, 4237–4246. [CrossRef]
20. Berlinger, F.; Gauci, M.; Nagpal, R. Implicit Coordination for 3D Underwater Collective Behaviors in a Fish-Inspired Robot Swarm. *Sci. Robot.* **2021**, *6*, eabd8668. [CrossRef]
21. Rahman, M.S. *Basic Graph Theory*; Springer: Berlin/Heidelberg, Germany, 2017; Volume 9.

22. Aldana, M.; Dossetti, V.; Huepe, C.; Kenkre, V.M.; Larralde, H. Phase Transitions in Systems of Self-Propelled Agents and Related Network Models. *Phys. Rev. Lett.* **2007**, *98*, 095702. [CrossRef]
23. Olfati-Saber, R. Flocking for Multi-Agent Dynamic Systems: Algorithms and Theory. *IEEE Trans. Autom. Control* **2006**, *51*, 401–420. [CrossRef]
24. Fu, X.; Zhang, Y.; Zhu, J.; Wang, Q. Bioinspired Cooperative Control Method of a Pursuer Group vs. a Faster Evader in a Limited Area. *Appl. Intell.* **2022**, *53*, 6736–6752. [CrossRef]
25. Qiu, H.; Duan, H. A Multi-Objective Pigeon-Inspired Optimization Approach to UAV Distributed Flocking among Obstacles. *Inf. Sci.* **2020**, *509*, 515–529. [CrossRef]
26. Yang, P.; Liu, M.; Peng, X.; Lei, X. Progress of Theoretical Modelling and Empirical Studies on Collective Motion. *Chin. Sci. Bull.* **2014**, *59*, 2464–2483. [CrossRef]
27. Duan, H.; Huo, M.; Shi, Y. Limit-Cycle-Based Mutant Multiobjective Pigeon-Inspired Optimization. *IEEE Trans. Evol.* **2020**, *24*, 948–959. [CrossRef]
28. Hemelrijk, C.K.; Hildenbrandt, H. Some Causes of the Variable Shape of Flocks of Birds. *PLoS ONE* **2011**, *6*, e22479. [CrossRef]
29. Ballerini, M.; Cabibbo, N.; Candelier, R.; Cavagna, A.; Cisbani, E.; Giardina, I.; Lecomte, V.; Orlandi, A.; Parisi, G.; Procaccini, A.; et al. Interaction Ruling Animal Collective Behavior Depends on Topological Rather than Metric Distance: Evidence from a Field Study. *Proc. Natl. Acad. Sci. USA* **2008**, *105*, 1232–1237. [CrossRef] [PubMed]
30. Chen, C.; Chen, G.; Guo, L. On the Minimum Number of Neighbors Needed for Consensus of Flocks. *Control Theory Technol.* **2017**, *15*, 327–339. [CrossRef]
31. Virágh, C.; Vásárhelyi, G.; Tarcai, N.; Szörényi, T.; Somorjai, G.; Nepusz, T.; Vicsek, T. Flocking Algorithm for Autonomous Flying Robots. *Bioinspir. Biomim.* **2014**, *9*, 025012. [CrossRef]
32. Xie, G.; Xu, H.; Li, Y.; Hu, X.; Wang, C.-D. Consensus Enhancement for Multi-Agent Systems with Rotating-Segmentation Perception. *Appl. Intell.* **2022**, *53*, 5750–5765. [CrossRef]
33. Yang, P.; Tang, Y.; Song, J. Self-Organized Fission/Fusion Method for Flocking System Based on Predictive Intelligence. *Control Decis.* **2018**, *33*, 2270–2276.
34. Alexander, R. Solving Ordinary Differential Equations i: Nonstiff Problems (e. Hairer, Sp Norsett, and g. Wanner). *Siam Rev.* **1990**, *32*, 485. [CrossRef]